The use of sulphur as a metallicity tracer in galaxies



Ángeles I. Díaz

Universidad Autónoma de Madrid
Institute of Astronomy Cambridge



ESTALLIDOS V: Star formation and metallicity

- Why sulphur? (Why not?)
- Low metallicity regions
- Abundance gradients
- High metallicity regions

Oxygen as abundance tracer in gaseous nebulae

- Oxygen is the most abundant element after Hydrogen and Helium.
- It is produced in high mass stars and hence it is returned to the ISM in a short time scale. Its abundance can be associated with “present day abundances”.



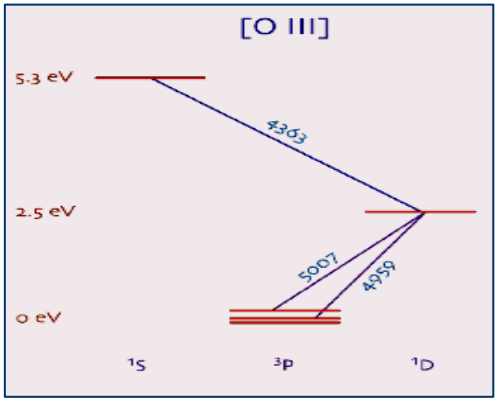
- Traditionally, the metallicity of gaseous nebulae has been traced by oxygen.
- Metallicity $\Rightarrow$ 12 + log (O/H)
- Solar metallicity $\Rightarrow$ 12 + log $(O/H)_{\odot}$ = 8.66 (Asplund et al. 2004)

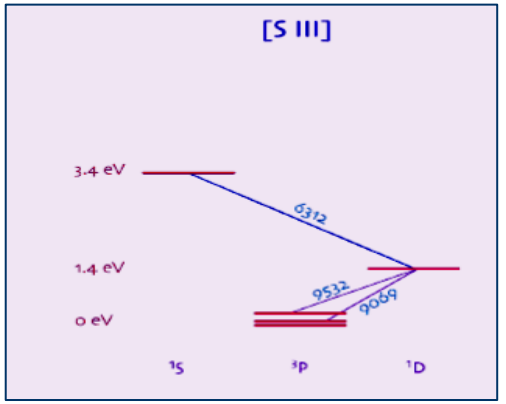
What about Sulphur?

- Sulphur is also produced in massive stars.
- Its yield is supposed to follow that of Oxygen
  $\Rightarrow$S/O ratio remains constant S/O $\cong$ -1.6.
- Although Sulphur is less abundant than Oxygen, in principle, ***it can be used as abundance tracer*** providing similar information.

Advantages of the use of Sulphur as abundance tracer

- The far read lines of [SIII] at λλ 6312, 9069, 9532 Å are analogous to those of [OIII] at λλ 4363, 4959, 5007 Å, but their emissivities are less dependent on T_e .



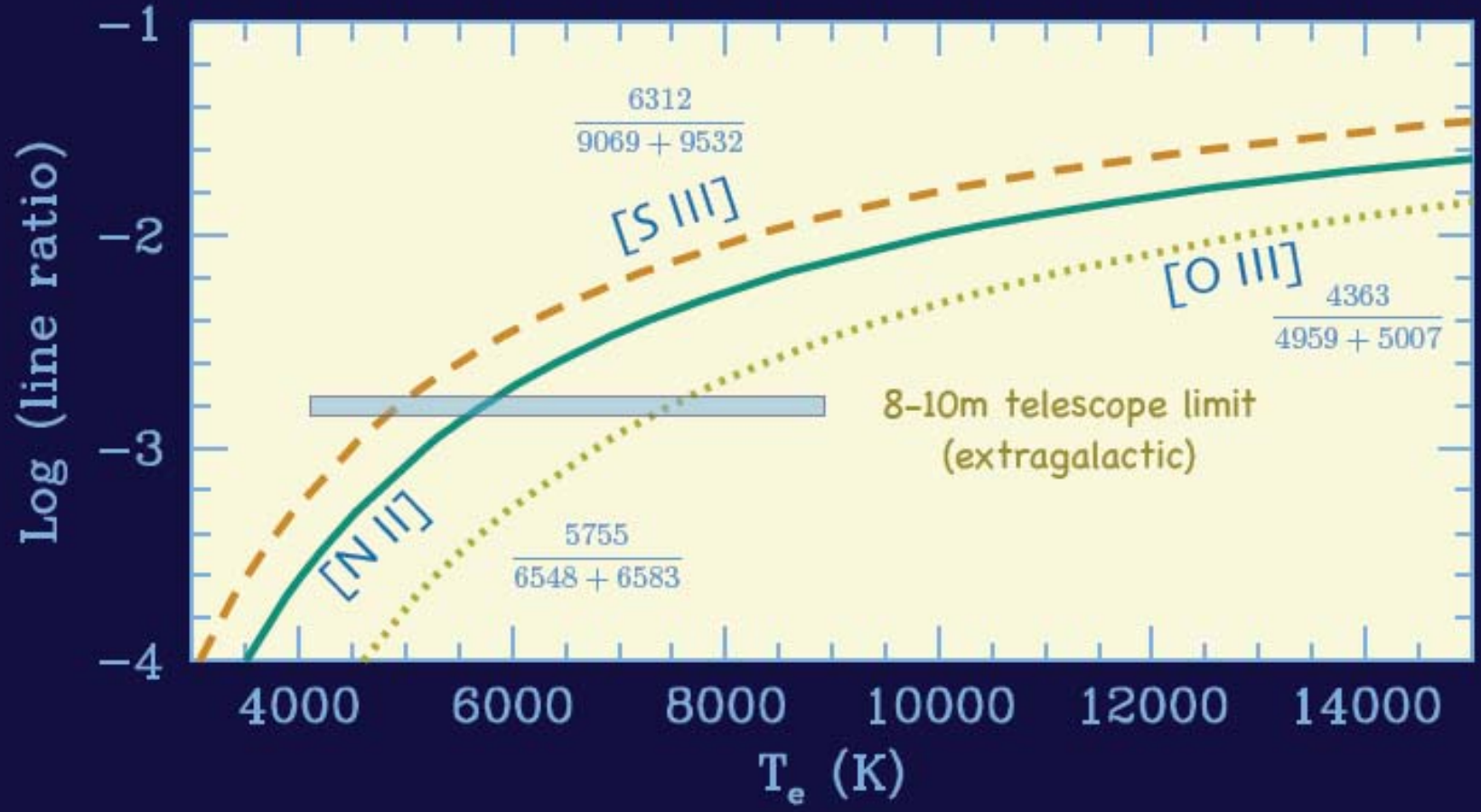


$$I_\lambda \propto N(X^{+i})\varepsilon_\lambda \quad \text{with} \quad \varepsilon_\lambda \propto \Omega(T) T_e^{-0.5} e^{-\frac{\chi_i}{kT_e}}$$

and $\chi(S^{2+}) < \chi(O^{2+})$

T[S III] = 4800
T[N II] = 5900 in M83 nucleus

Bresolin, Schaerer, Gonzalez
Delgado & Stasinska (2005)



Direct determination of abundances

Knowledge of line electron temperatures is required

Oxygen

- T_e([OIII] is derived from the ratio of auroral to nebular lines at λλ 4363 and 4959, 5007 Å
- Most of the O is in the form of O^+ and O^{2+}. Their relative contribution depends on the degree of ionization of the nebula.
- Only for exceptionally high excitation objects, those showing HeII emission at λ 4686 Å, there is a small contribution by O^{3+}.

Sulfur

- T_e([SIII]) is derived from the ratio of auroral to nebular lines at λλ 6312 and 9069, 9532 Å.
- Most of the S is also in the form of S^+ and S^{2+}, but in most cases S^{2+} is dominant.
- A certain contribution by S^{3+} is expected in high excitation objects for which ICF have to be derived.

Ionization structure

- The T across a nebula is not constant $\Rightarrow$ different ions are formed in regions with different T.
- A certain ionization structure has to assumed for the nebula. Two-zone approximation



high ionization zone	low ionization zone
O^{2+}, Ne^{2+}	O^{+}, Ne^{+},S^{+},N^{+}
(inner)	(outer)

- For O, T_e([OII] is predicted from T_e([OIII] with the help of photo-ionization models.

$$T_e([OII]) = 0.70 T_e([OIII]) + 3000K$$ *(Stasińska 1980)*

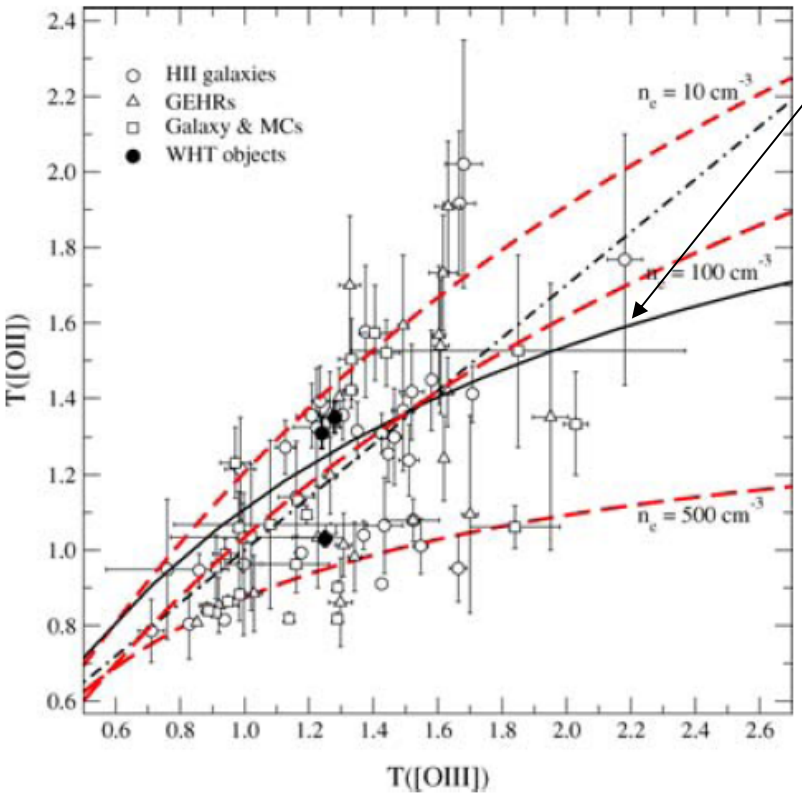


Figure 8. Relation between $T([O\,II])$ and $T([O\,III])$ for the observed objects (solid circles) and H II galaxies (open circles), GEHRs (upward triangles) and diffuse H II regions in the Galaxy and the Magellanic Clouds (squares) from Pérez-Montero & Díaz (2005). The dashed lines correspond to photoionization models from Pérez-Montero & Díaz (2003) for electron densities n_e = 10, 100 and 500 cm^{-3}. The model sequences from Stasińska (1980; solid line) and Stasińska (1990; dot–dashed line) are also shown. The temperatures are in units of 10^4 K.

Pérez-Montero & Díaz 2003

However, T([OII]) depends on electron density.

The relation between T([OII]) and T([OIII]) is not so straightforward.

Empirically derived relation shows a large scatter.

The determination of O^+/H^+ ratio often carries a large uncertainty

S^{2+} seems to originate in an intermediate excitation zone. $T_e([SIII])$ can also be predicted from $T_e([OIII])$ using photo-ionization models.

$$T_e([SIII]) = 0.83T_e([OIII]) + 1700K$$

(Garnett 1992)

Assuming $T_e([SII]) \cong T_e([OII])$ provides a relation between $T_e([SII])$ and $T_e[SIII]$ as:

$$T_e([SII]) = 0.88T_e([SIII]) + 1560K$$

$$T_e([SII]) \approx T_e([SIII])$$

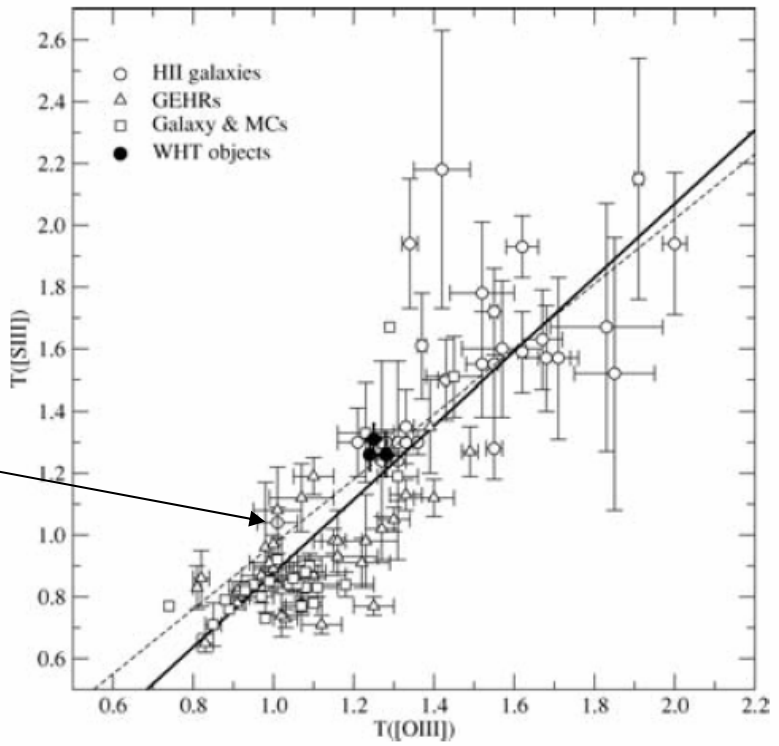


Figure 7. Relation between $T([S\,III])$ and $T([O\,III])$ for the observed objects (solid circles), and H II galaxies (open circles), GEHRs (upward triangles) and diffuse H II regions in the Galaxy and the Magellanic Clouds (squares), for which data on the auroral and nebular lines of [O III] and [S III] exist (see Pérez-Montero et al. 2006). The temperatures are in units of 10^4 K.

Oxygen: Large uncertainties in T_e([OII]) can translate into large uncertainties in final O/H values, more important in low excitation objects where $O^+/O^{2+} > 1$.

Sulphur: Uncertainties in T_e([SII] are not important since even in low excitation objects $S^+/S^{2+} < 1$.
For instance, for the low excitation region CCM10 in M51 $O^+/O^{2+} \cong 6$, while $S^+/S^{2+} \cong 0.3$
(Bresolin, Garnett & Kennicutt 2004)

In fact, in most cases, the assumption of Te([SII]) ~ Te([SIII]) can be made.

Also, T_e([SIII]) is probably more representative of the average T in the nebula than either T_e([OII] or T_e([OIII])

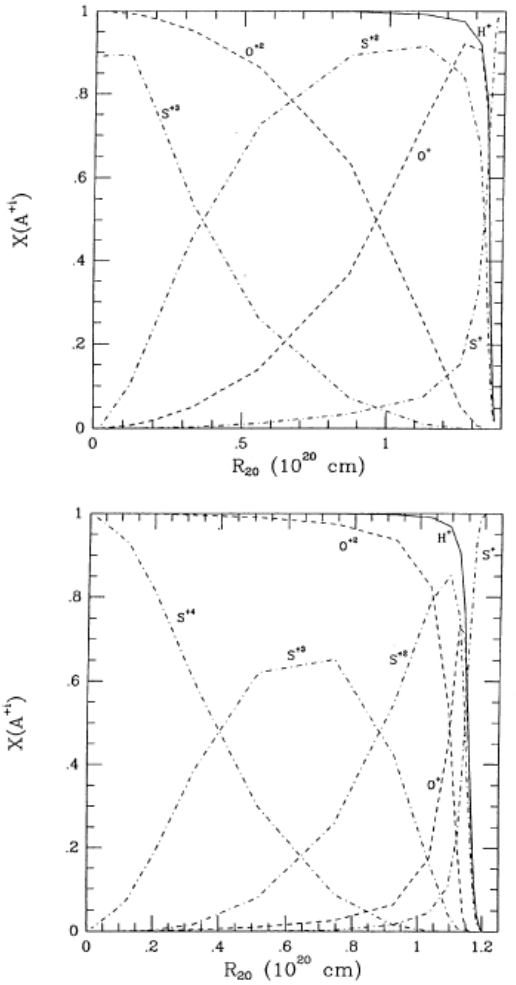
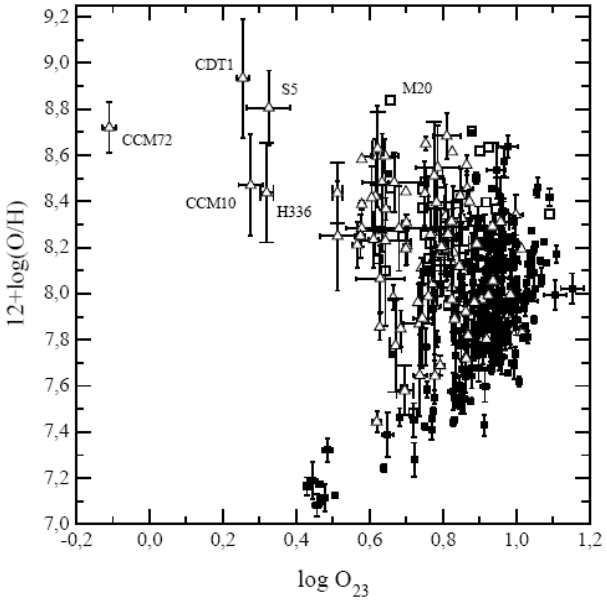


FIG. 2. The ionization structure for sulfur and oxygen in two model nebulae. (a) Model with $T_{\rm eff} = 40\,000$ K and solar abundances. (b) Model with $T_{\rm eff} = 50\,000$ K and one-tenth solar abundances. S^{+2} is abundant in both the O^+ and O^{+2} zones, demonstrating that ionization potentials can be misleading as a guide to intuiting ionization structure.

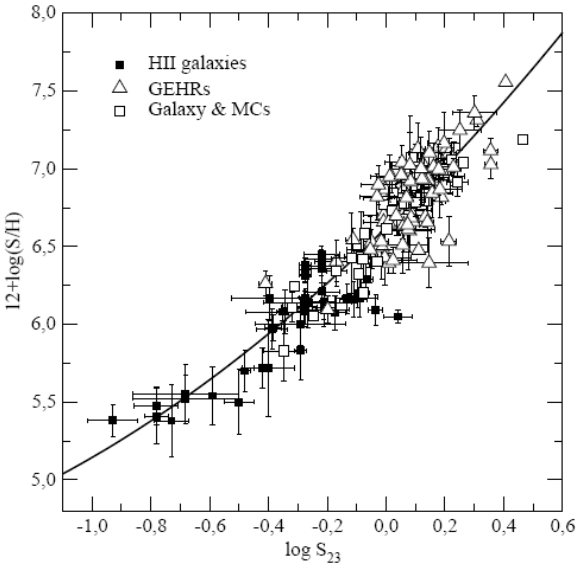
Garnett 1998

Empirically derived abundances

- Due to the increasing importance of O as a coolant from 12+log(O/H) ~ 8.2 upwards, the strong-line empirical calibration for O is two-folded.

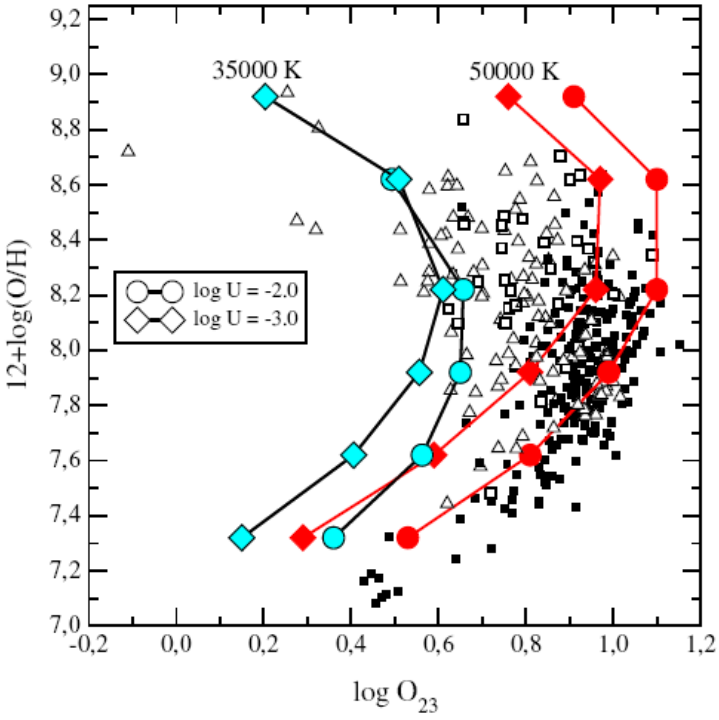


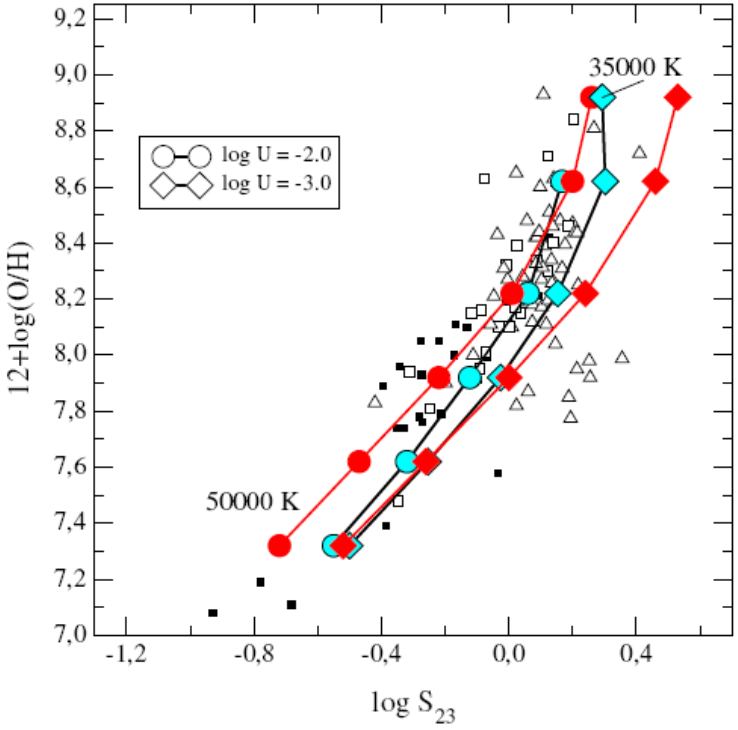
- S being less abundant than O and its emission lines being at longer λ, its relevance as cooling agents starts at lower temperatures (higher abundances ~ solar).



Pérez-Montero & Diaz 2005

Also “second order parameters” (U, T_{ion}) less important for the S calibration than than for the O calibration.



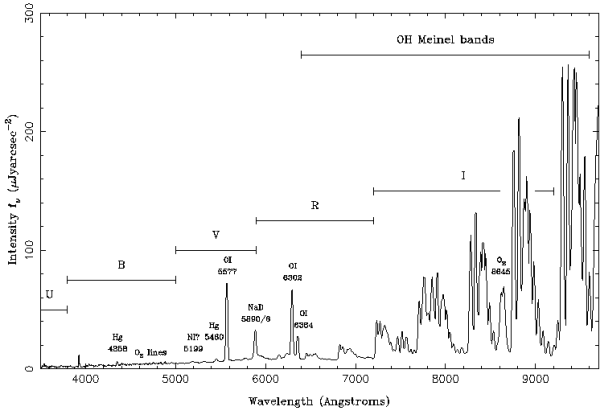


Pérez-Montero & Diaz 2005

The sky in the near infrared

- In the far red the night sky emission is important and has to be carefully removed. Moderate spectral resolution (R ~ 2500 – 4000) improves the substraction.

- Also, water absorption bands can be prominent. It can be removed with the help of observations of a star before and/or after the object exposure.



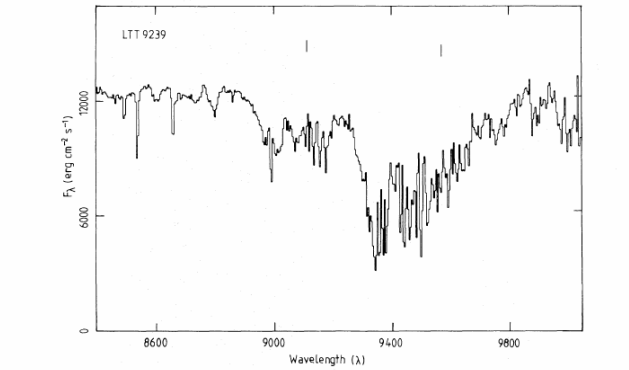


Figure 1. The atmospheric absorption features in the spectrum of the standard star LTT 9239. The wavelengths of the [S III] λλ 9069, 9532 lines are marked to show their positions relative to the underlying atmospheric absorption bands. A redshift of 1000 km s^{-1}, typical of the Liner galaxies observed, has been applied.

Data improvement over time

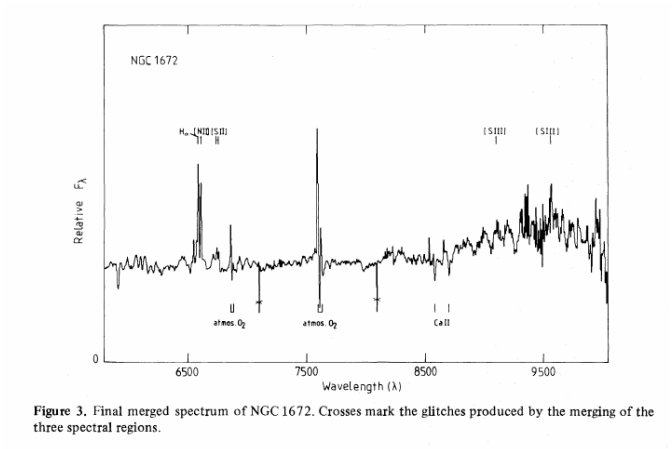
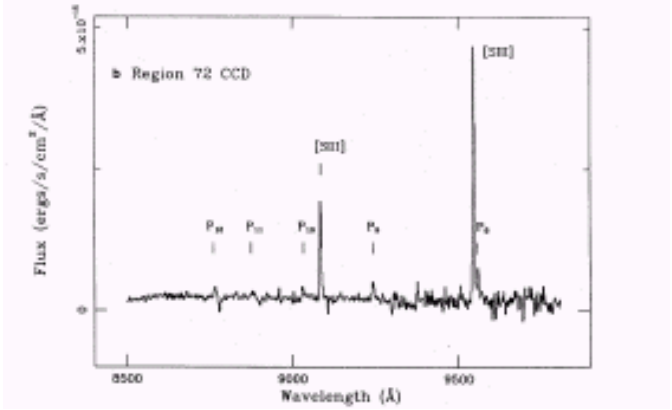


Figure 3. Final merged spectrum of NGC 1672. Crosses mark the glitches produced by the merging of the three spectral regions.

Díaz, Pagel & Wilson 1985



Díaz et al. 1991

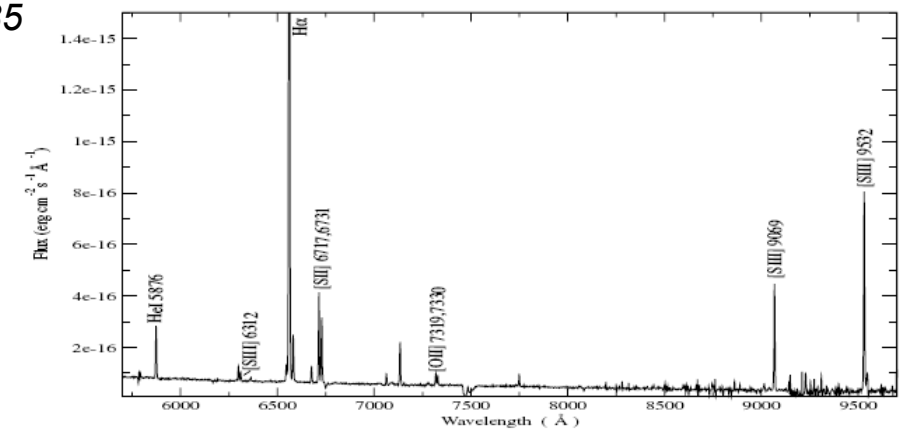
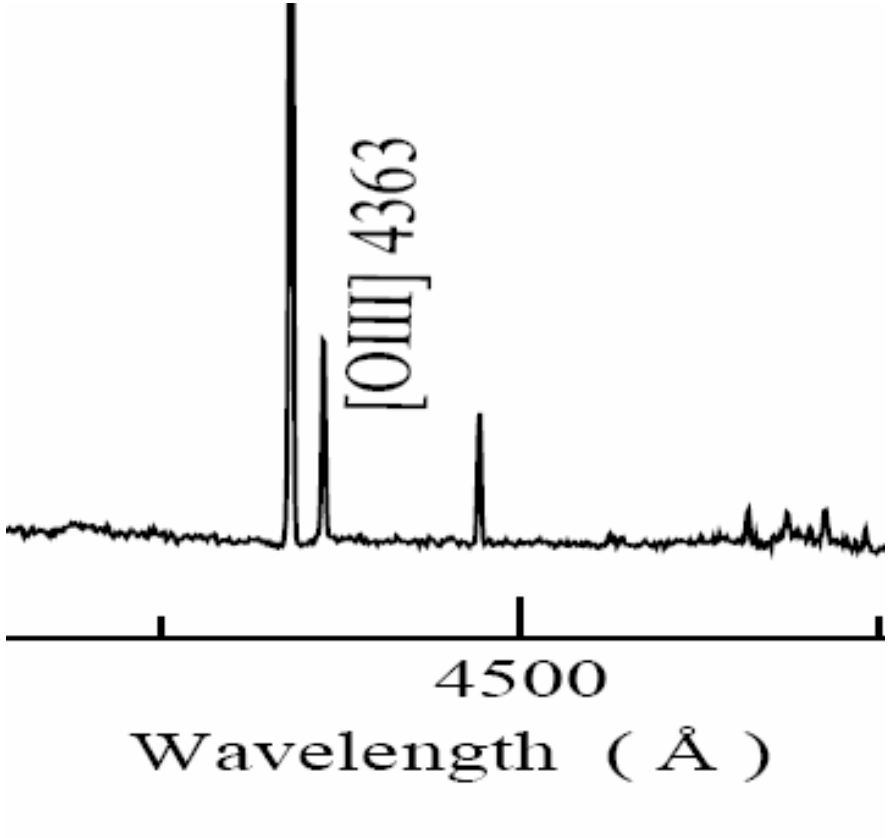
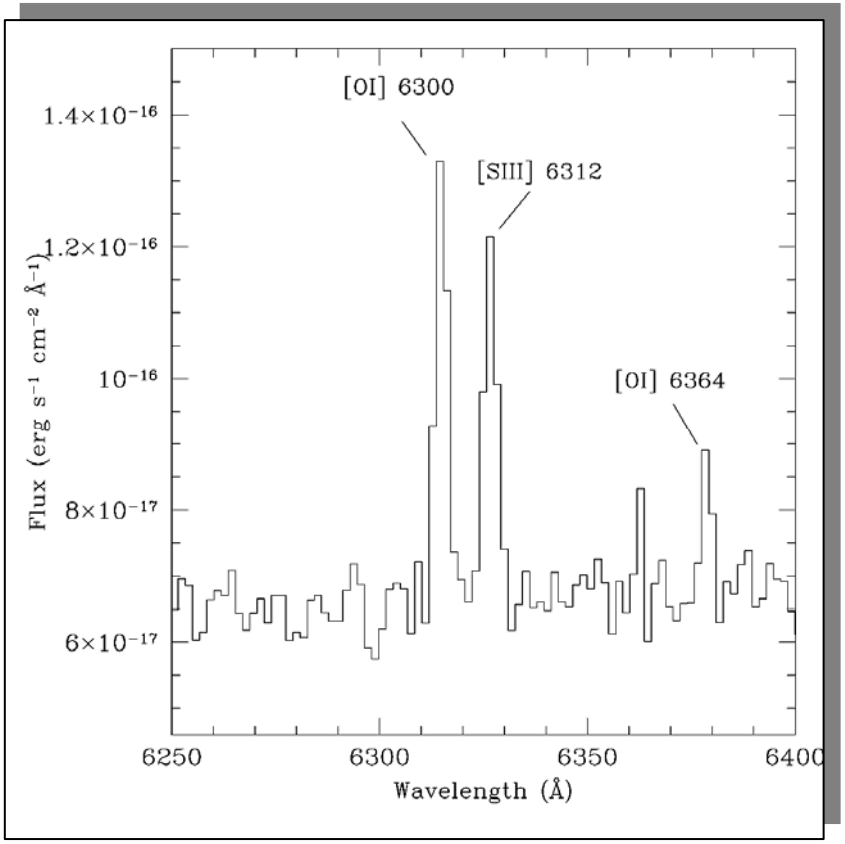


Figure 2. WHT spectra of SDSS J003218.60+150014.2 in the rest frame for the two observed ranges.

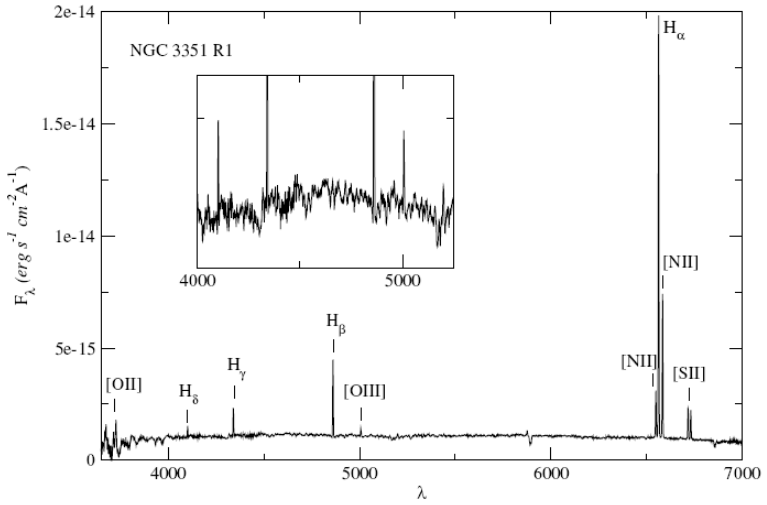
Hägele et al. 2007

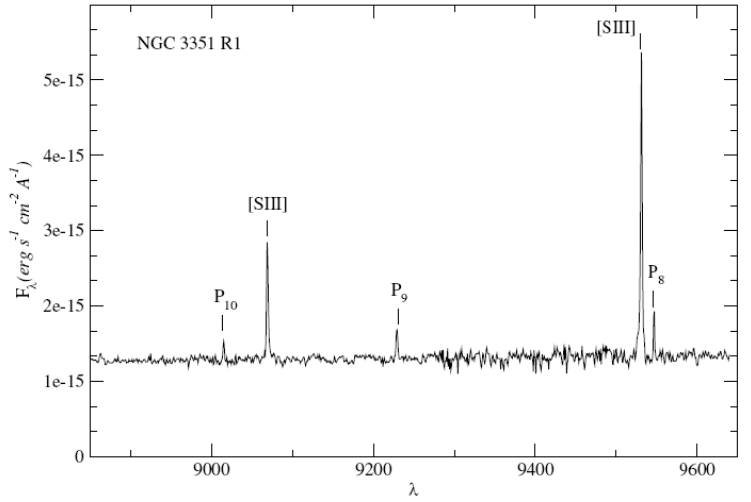

[OIII] 4363
4500
Wavelength (Å)


[OI] 6300
[SIII] 6312
[OI] 6364
1.4×10⁻¹⁶
1.2×10⁻¹⁶
10⁻¹⁶
8×10⁻¹⁷
6×10⁻¹⁷
Flux (erg s⁻¹ cm⁻² Å⁻¹)
6250
6300
6350
6400
Wavelength (Å)

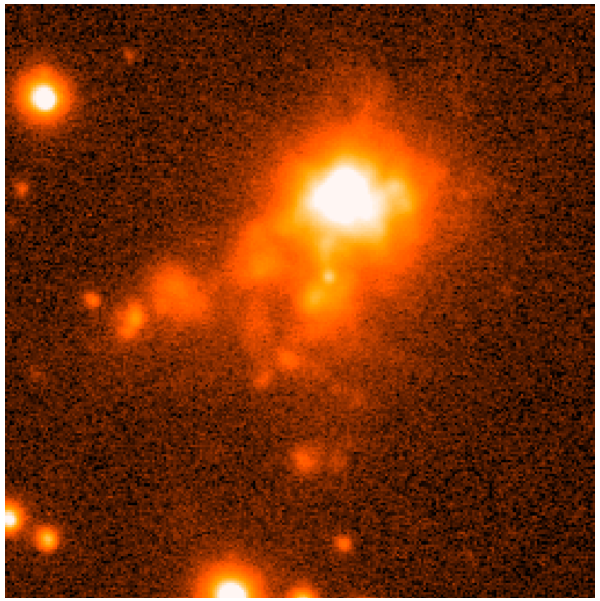
Observational advantages of S

- Less contamination from stellar absorption lines from metals (there are many more lines in the blue)
- Less contribution to the Balmer H lines from stellar absorption.
- Less importance of reddening.
- [SII] and [SIII] can be measured relative to nearby H lines, minimizing the effects of reddening.
- [SIII] lines clearly detected at high abundances where “strong” [OIII] lines are very weak.





Low metallicity: HII galaxies

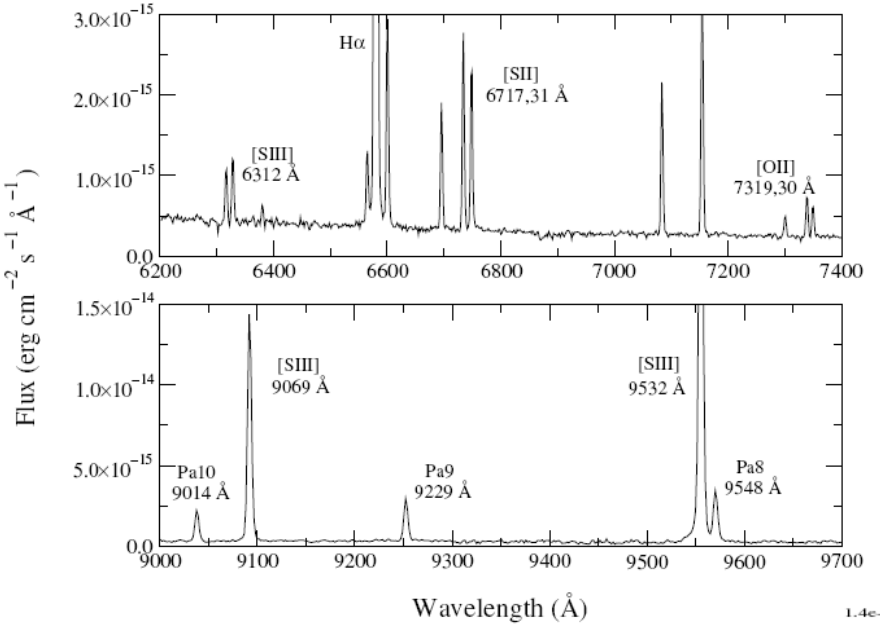


Sample analyzed comprises data from:

- Pérez-Montero & Díaz (2003; INT)
- Hägele et al. (2006; WHT)
- Hägele et al. (2007; CAHA)
- Kehrig et al. (2006; ESO 1.52m La Silla)
- Izotov et al. (2006; SDSS)

Total number of objects ~ 40 + 110 (SDSS)

Representative spectra



IIZw40
Pérez-Montero & Díaz (2003)

SDSS JD0321860+150014.2
Hägele et al. (2006)

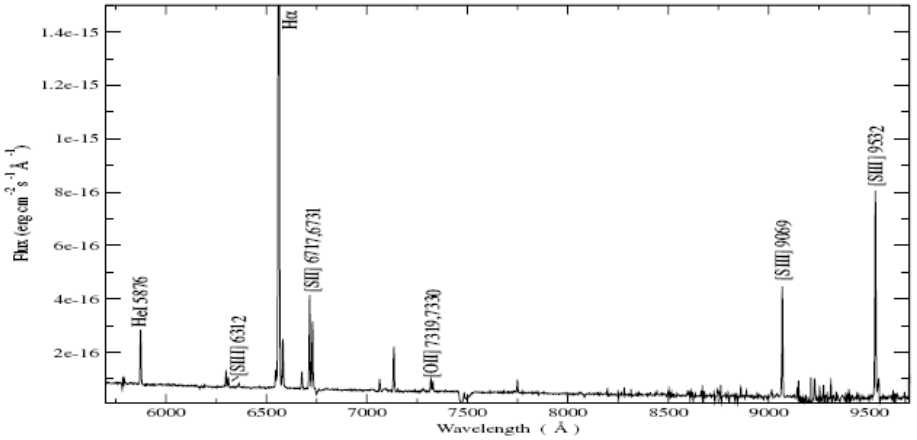


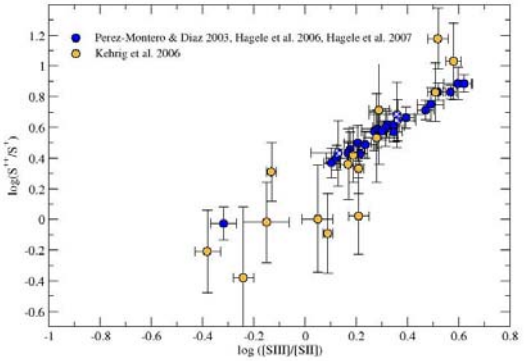
Figure 2. WHT spectra of SDSS J003218.60+150014.2 in the rest frame for the two observed ranges.

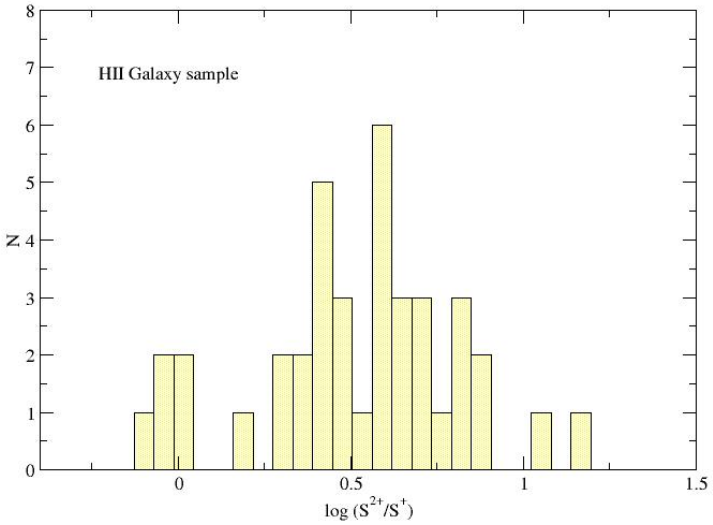
Methodology: Direct abundance determination

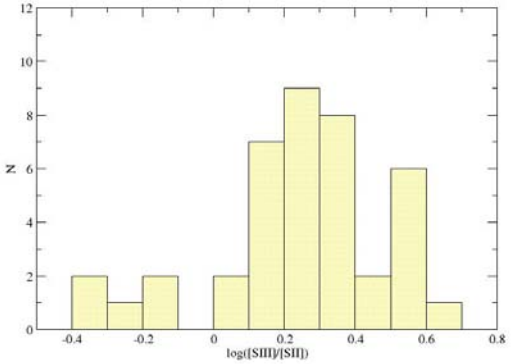
- Abundances derived from observations in the 6000 – 10000 Å spectral region.
- T_e([SIII]) derived from the I(6312)/I(9069+9532) line intensity ratio.
- Assume T_e([SII]) ~T_e([SIII]).
- Calculate S^+/H^+ and S^{2+}/H^+ ratios.
- Estimate ICF(contribution from S^{3+}) from the [SIII]/[SII] ratio.
- Calibrate the $(S^+ + S^{2+})/H^+$ and S/H abundance ratios.

Results

- $5 < (S^{+}+S^{2+})/H^{+} < 7$
- For most objects $S^{2+}/S^{+} > 1$
- [SII]/[SIII] maps the S^{+}/S^{2+} ratio





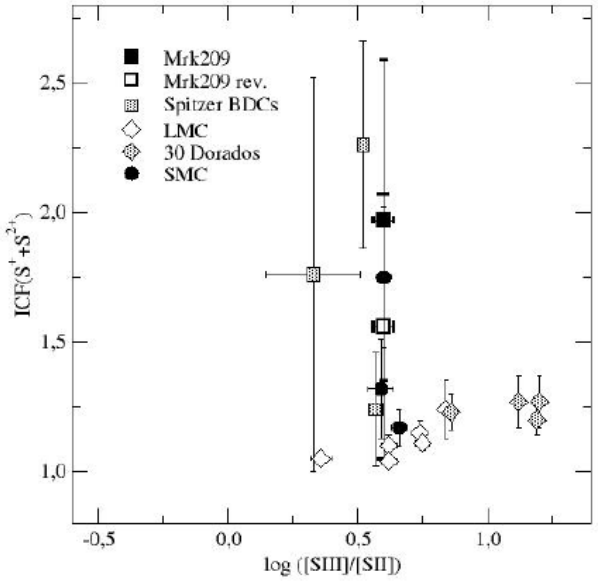


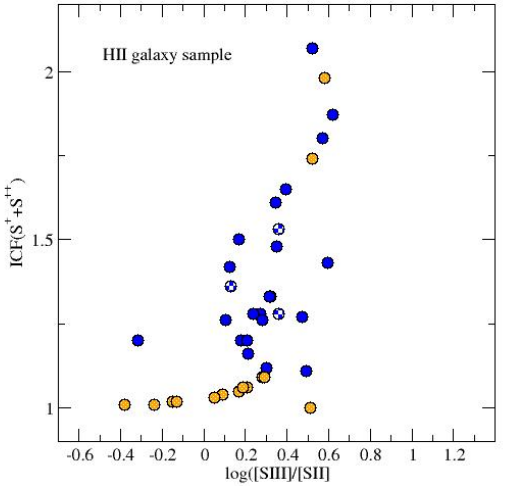
Ionization correction factors (ICF)

$$\frac{N(S)}{N(H)} = ICF(S^+ + S^{2+}) \cdot \frac{N(S^+ + S^{2+})}{N(H^+)}$$

The relation by Barker (1980) based on the photo-ionization models of Stasińska (1978), with α= 2.5 has been used.

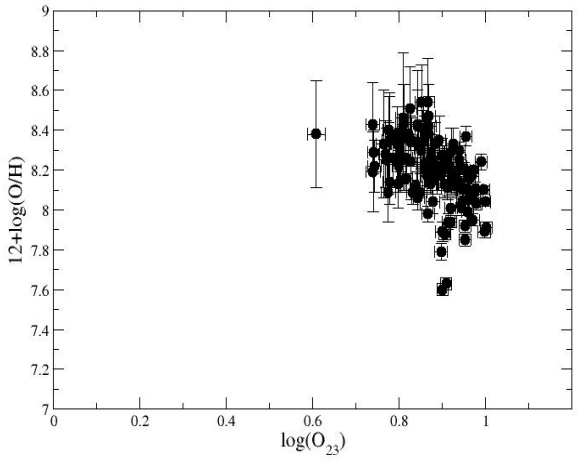
$$ICF(S^+ + S^{2+}) = \left[1 - \left(1 - \frac{N(O^+)}{N(O)}\right)^{\alpha}\right]^{-1/\alpha}$$

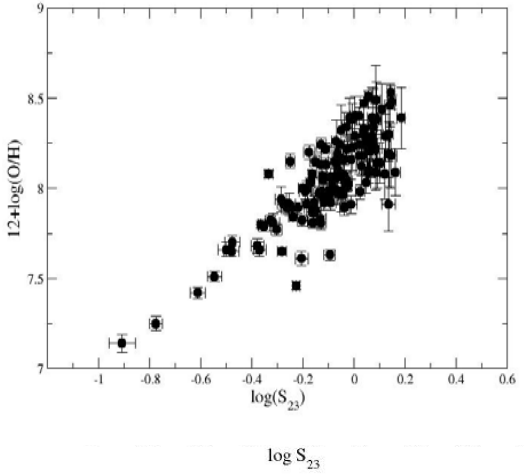




In order to improve on the determination of ICF for S, data on the IR 10.4 μm [SIV] line are needed

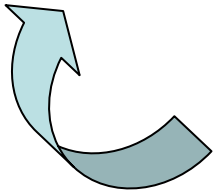
The empirical S calibration

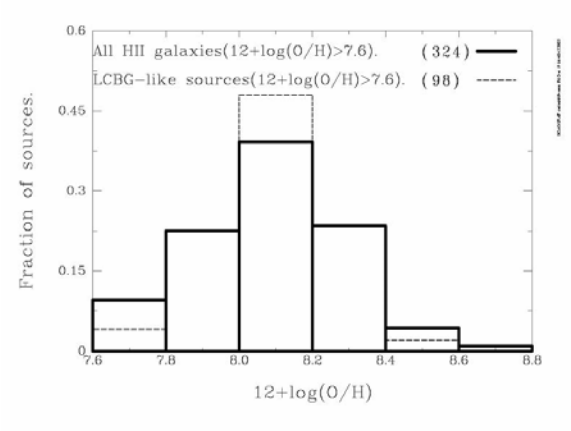


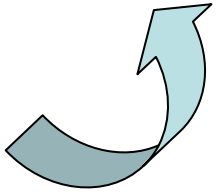


O_{23}

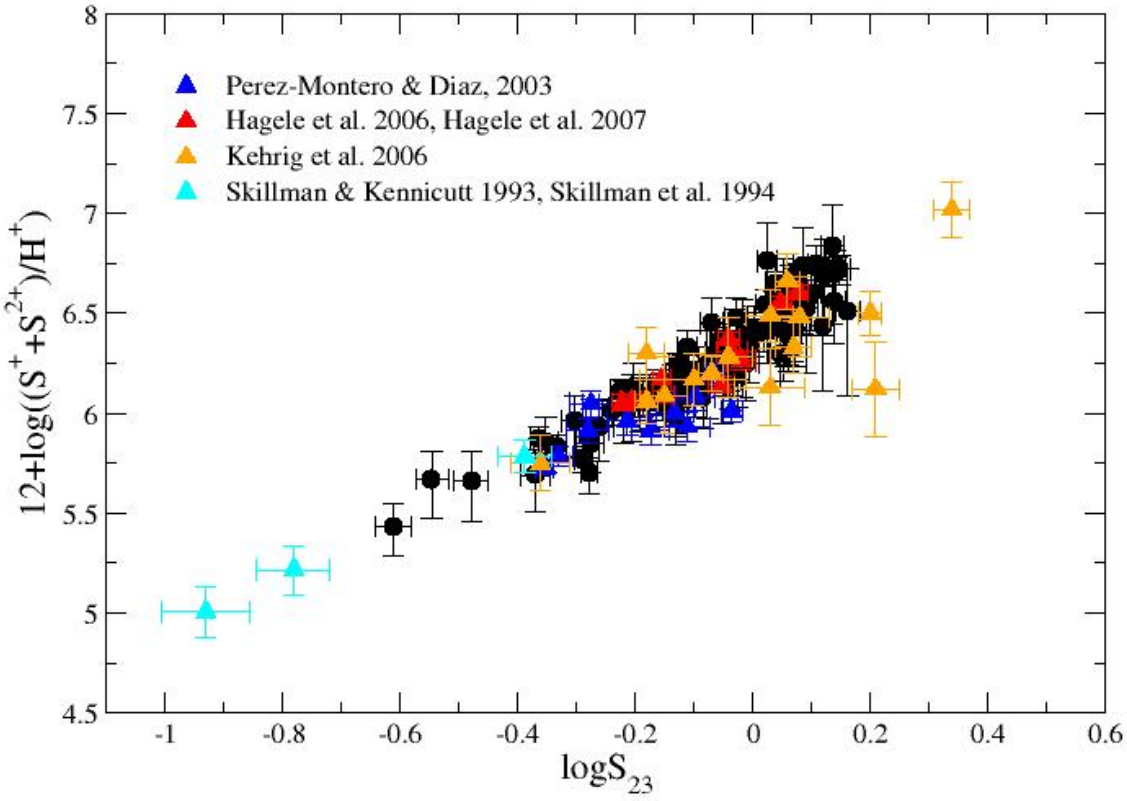
S_{23}





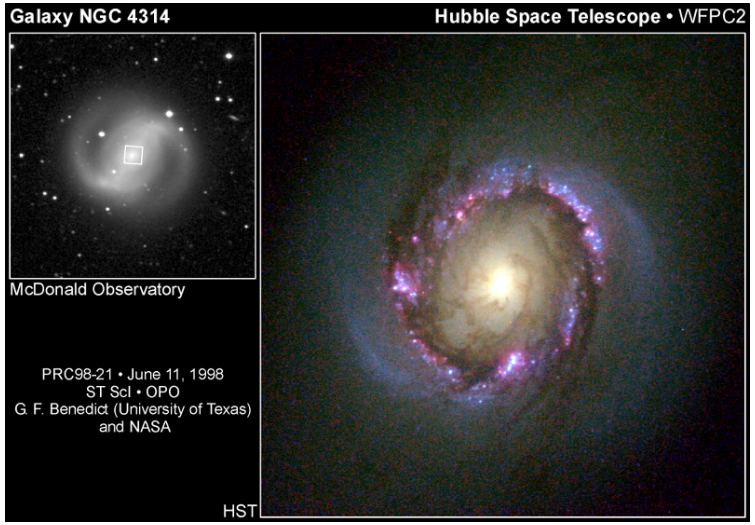


Empirical calibration with SDSS data



High metallicity regions: CNSFR

CNSFR in early type galaxies are expected to be of high metallicity, as corresponds to their position near the galactic bulge.



Sample analyzed comprises CNSFR in NGC 2903, NGC 3351 and NGC 3504 from:

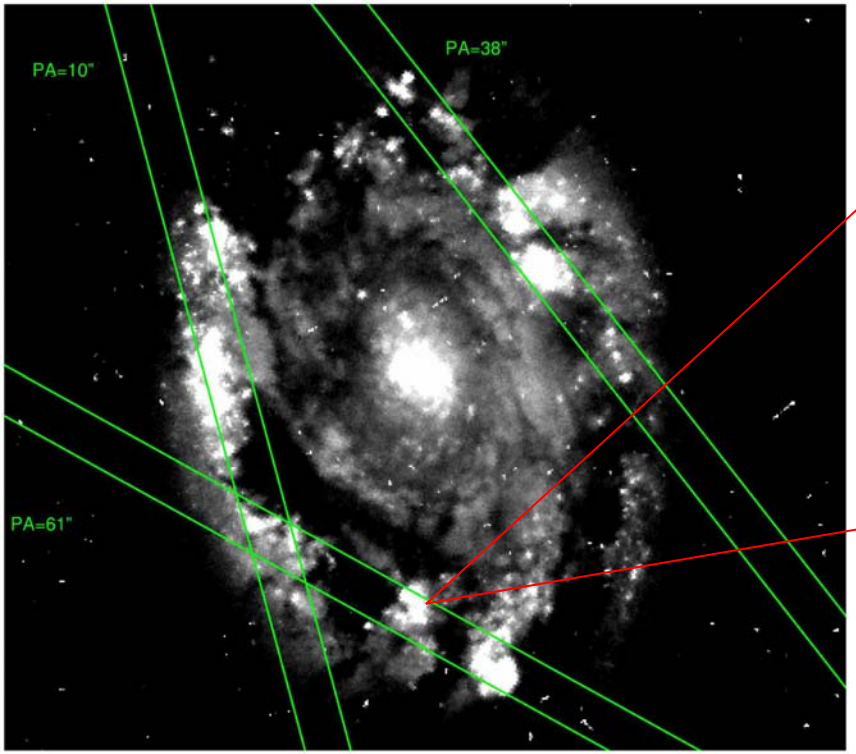
- Díaz et al. (2007)

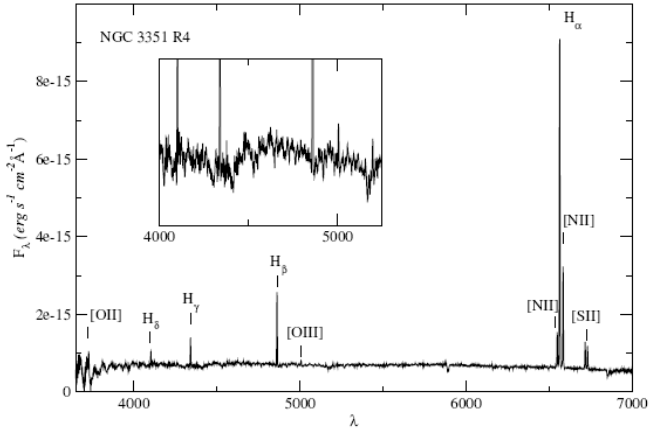
High metallicity HII regions from:

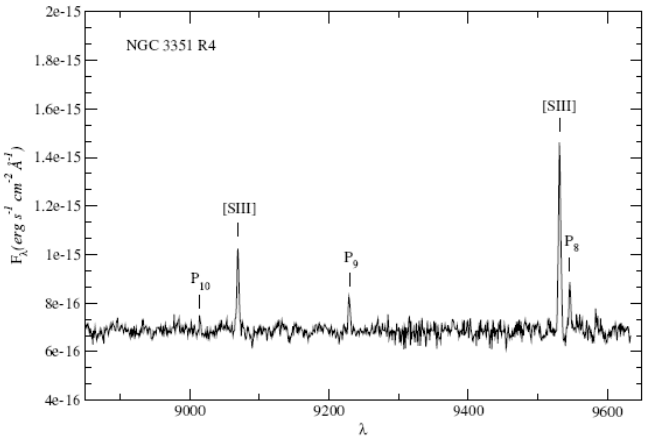
- Díaz et al. (2000)
- Castellanos et al. (2002)
- Bresolin, Garnett & Kennicutt (2004)
- Bresolin et al. (2005)

Representative spectra

NGC 3351

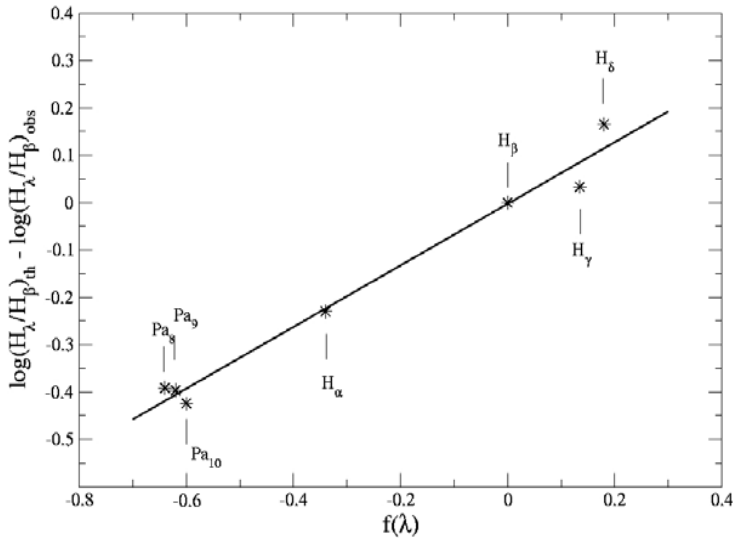




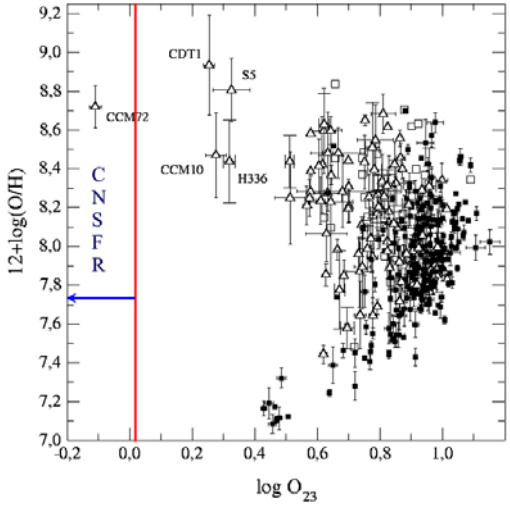


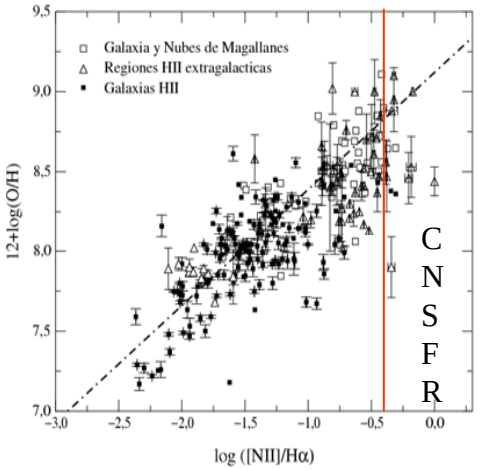
Underlying stellar absorption

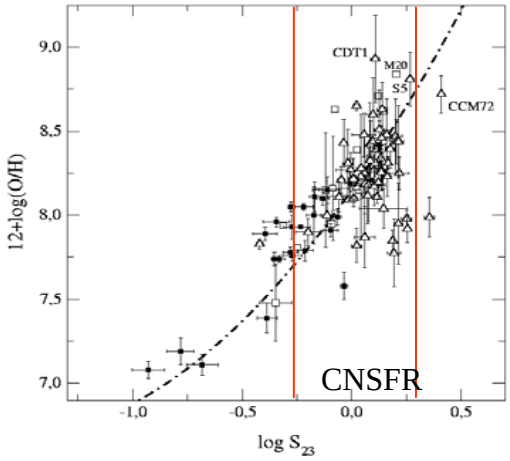
- Stellar absorption lines are very prominent since the regions are close to the galactic bulge. It is necessary to subtract the absorption component.
- This has been done for the Balmer lines, but the absorption is also important at the vawelengths of the [OIII] lines.

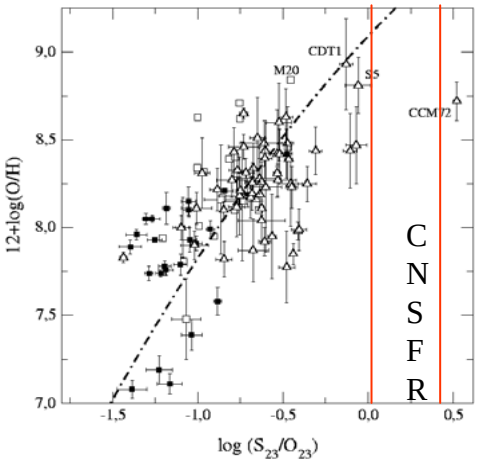


Empirical abundance indicators





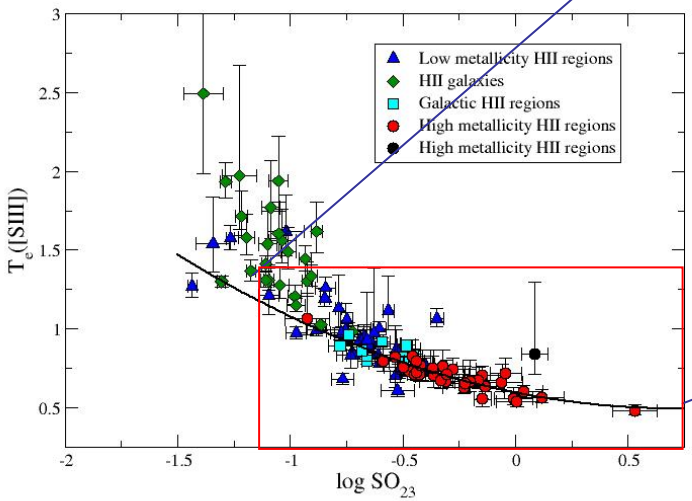


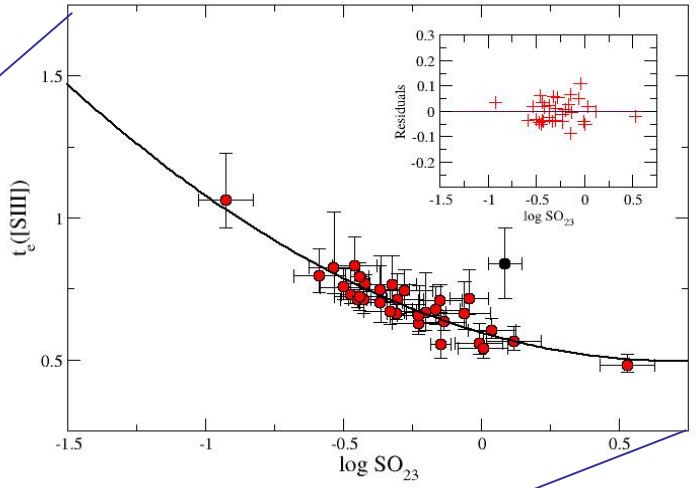


T_e([SIII]) calibration

T_e([SIII] can be calibrated in terms of the empirical parameter

$SO_{23} = S_{23}/O_{23}$





Then, ionic abundances are derived

Results

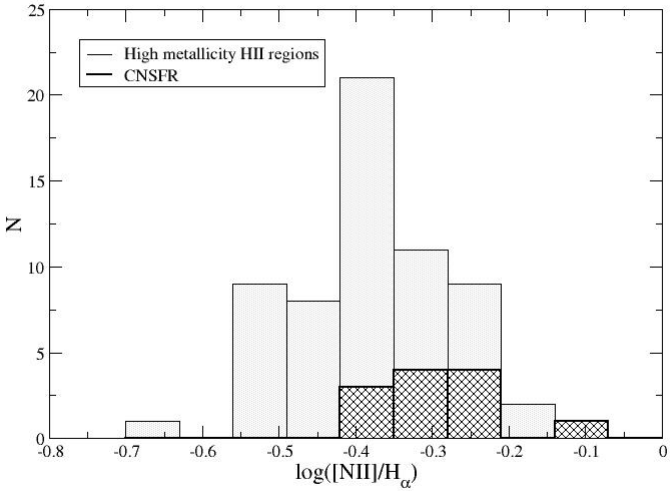
Table 8. Derived lectron densities, electron temperatures and ionic abundances from sulphur lines in our observed CNSFR.

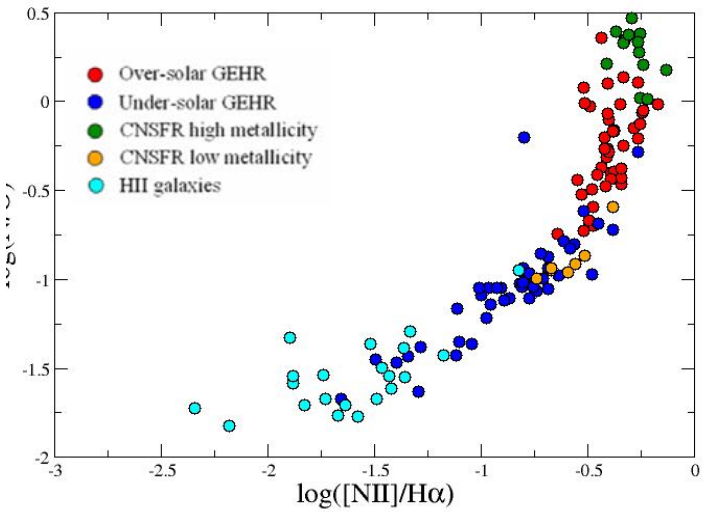
Galaxy	Region	n_e (cm^{-3})	T_e([SIII]) (K)	12+log (S^+/H^+)	12+log (S^{2+}/H^+)	12+log[(S^++S^{2+})/H]$^+$
NGC 2903	R1+R2	280 ± 90	5731 ± 188	6.83 ± 0.04	6.50 ± 0.05	7.01 ± 0.05
	R3	230 ±135	5737 ± 210	6.91 ± 0.06	6.60 ± 0.06	7.09 ± 0.06
	R4	270 ±120	6660 ± 331	6.68 ± 0.06	6.21 ± 0.08	6.81 ± 0.06
	R6	250 ± 80	5413 ± 221	6.97 ± 0.05	6.64 ± 0.06	7.14 ± 0.05
NGC 3351	R1	360 ± 80	5683 ± 188	6.74 ± 0.04	6.75 ± 0.05	7.05 ± 0.04
	R2	440 ±110	5405 ± 210	6.90 ± 0.05	6.65 ± 0.06	7.09 ± 0.05
	R3	430 ± 70	5399 ± 210	6.84 ± 0.04	6.83 ± 0.05	7.14 ± 0.05
	R4	310 ±120	5390 ± 271	6.87 ± 0.06	6.64± 0.07	7.07 ± 0.07
	R5	360 ±230	6177 ± 286	6.78 ± 0.07	6.49 ± 0.09	6.97 ± 0.08
	R6	360 ±170	6297 ± 295	6.49 ± 0.06	6.20 ± 0.07	6.67 ± 0.07
	R7	410 ±100	5537 ± 220	6.80 ± 0.05	6.52 ± 0.07	6.99 ± 0.06
NGC 3504	R3+R4	370 ± 60	6288 ± 170	6.86 ± 0.03	6.77 ± 0.03	7.12 ± 0.03

S abundances are found to be 6.67 < 12+log(S/H) < 7.14

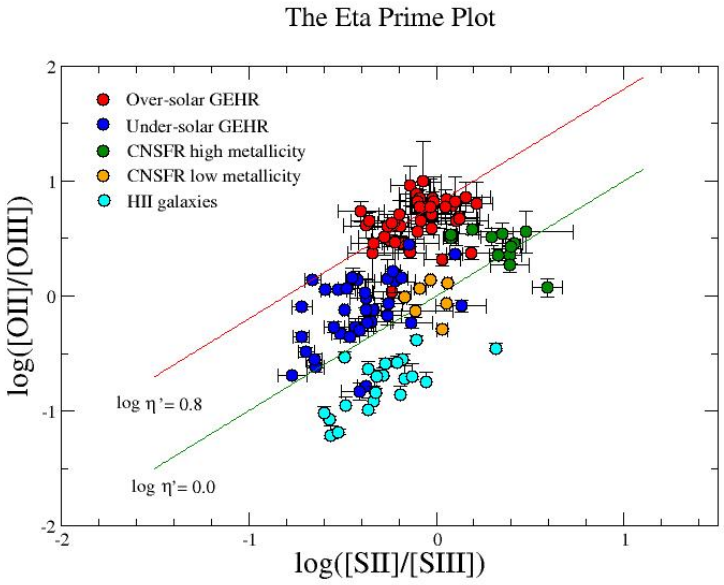
Corresponding O abundances are found to be 8.42 < 12+log(O/H) < 8.85

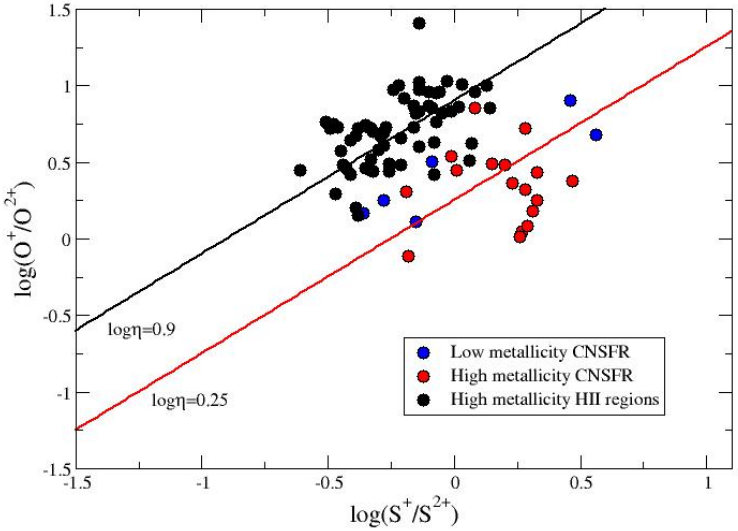
However, N/O seems to reach the highest observed values, which would point to higher O abundances



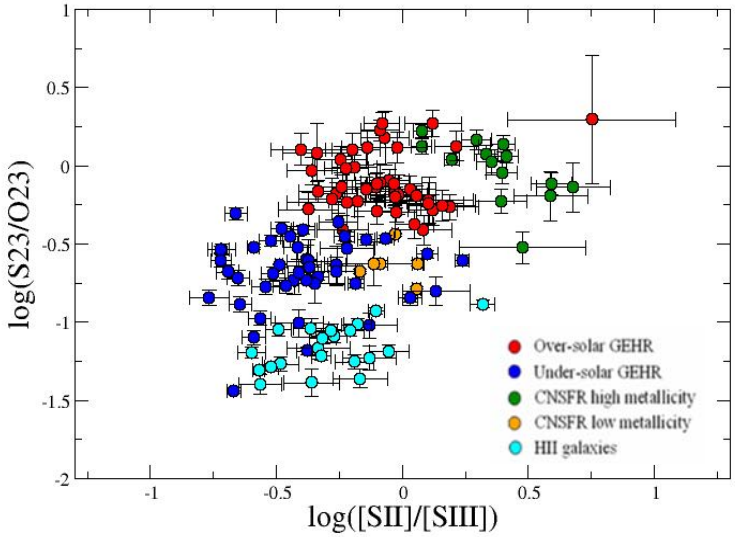


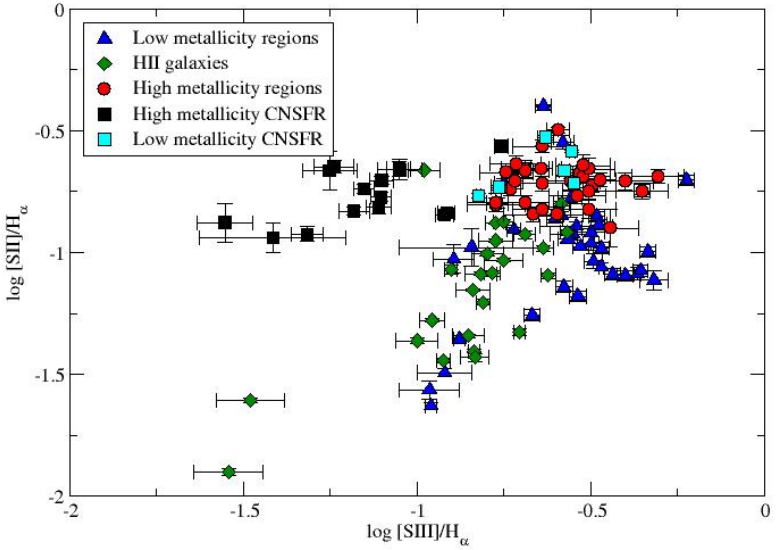
Ionising radiation





[SIII] lines too weak in high metallicity regions?





Similar to what is found for the inner region of M 101?

Metallicity gradients



Sample analyzed comprises HII regions in NGC 101 from:

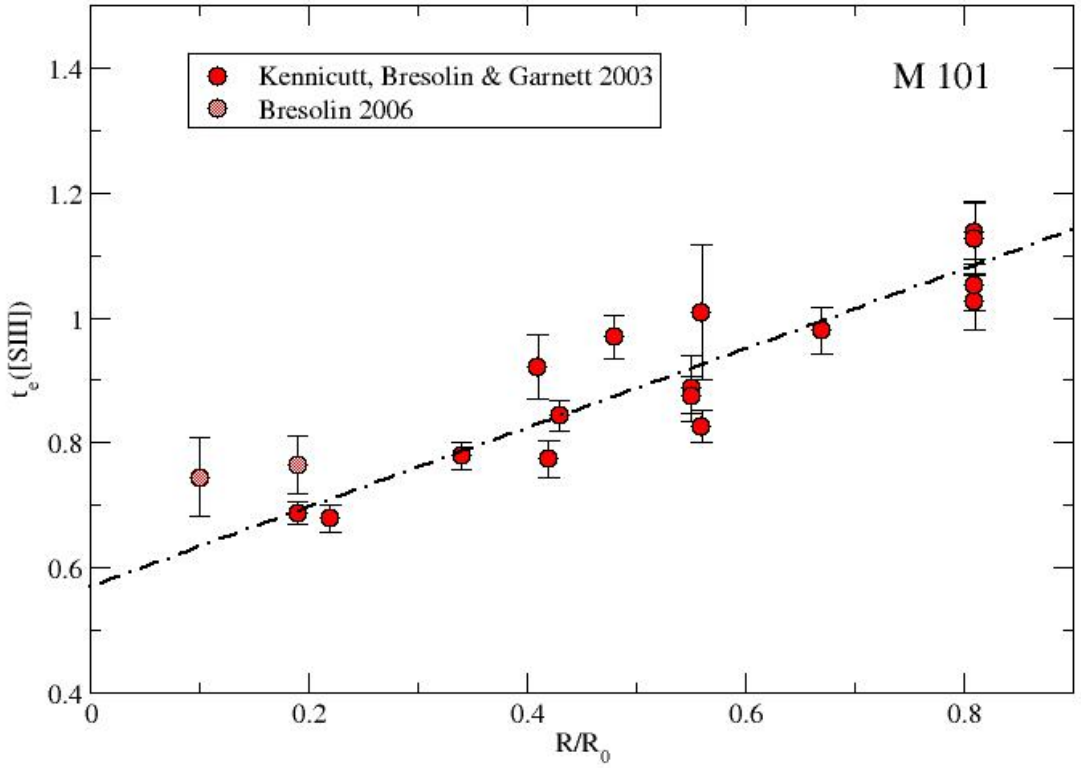
- Kennicutt, Bresolin & Garnett (2003)
- Bresolin (2006)

HII regions in NGC 2403 from:

- Garnett et al. (1997)

The analysis has been performed as explained before for the case of HII galaxies using the spectral region between 6000 and 10000 Å.

T_e([SIII]) gradient



$(S^{+}+S^{++})/H^{+}$ gradient

O/H gradient

Kennicutt, Bresolin & Garnett (2004)

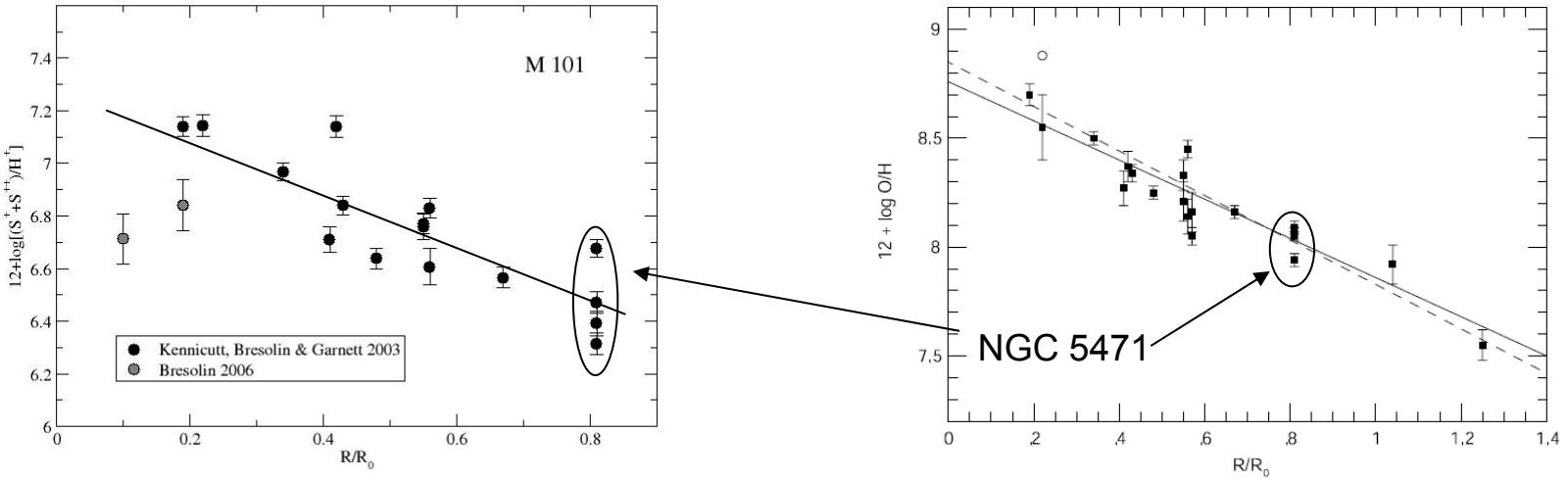
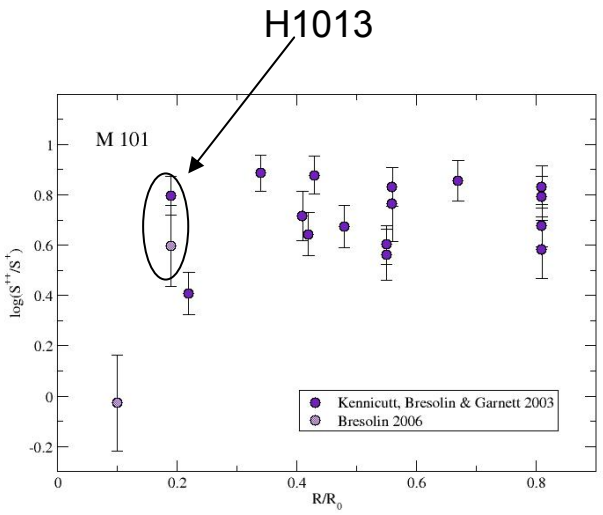
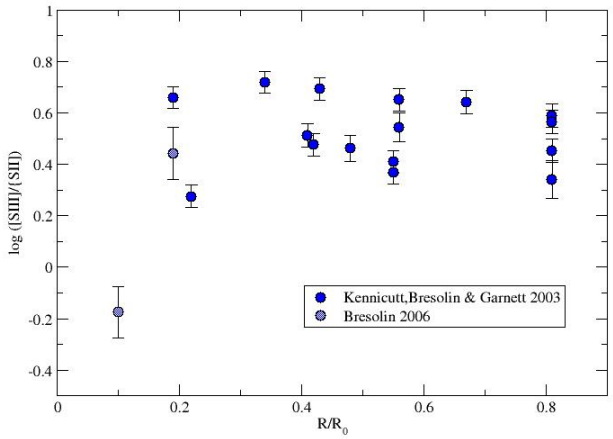
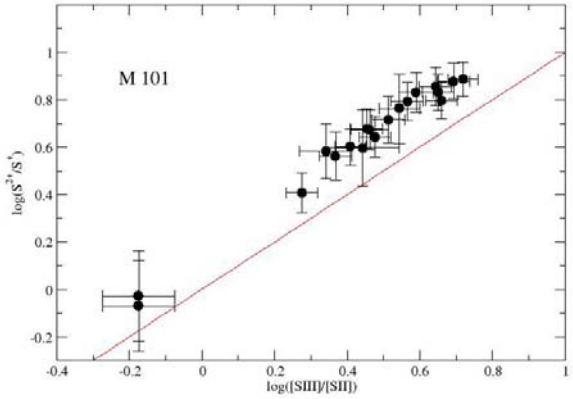


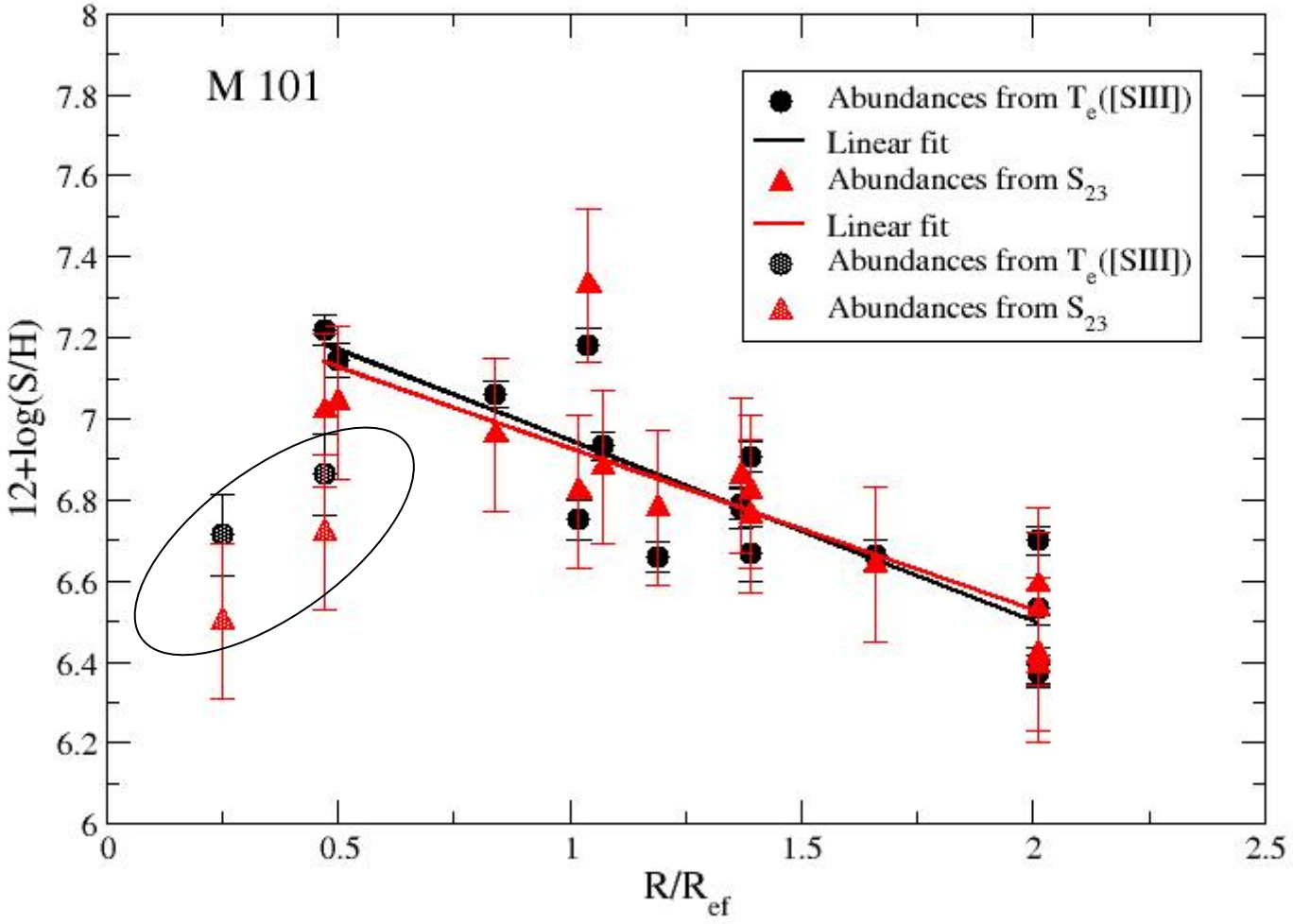
FIG. 6.—Oxygen abundance gradient in M101 from our 20 H II regions with electron temperature measurements. The linear fit to the data given by eq. (5) is shown by the solid line. The open circle is the abundance for H336 obtained by Kinkel & Rosa (1994). The dashed line shows the resulting fit if we use this point instead of our measurement, as given by eq. (6).


H1013
M 101
log(S^{++}/S^{+})
R/R$_0$
Kennicutt, Bresolin & Garnett 2003
Bresolin 2006

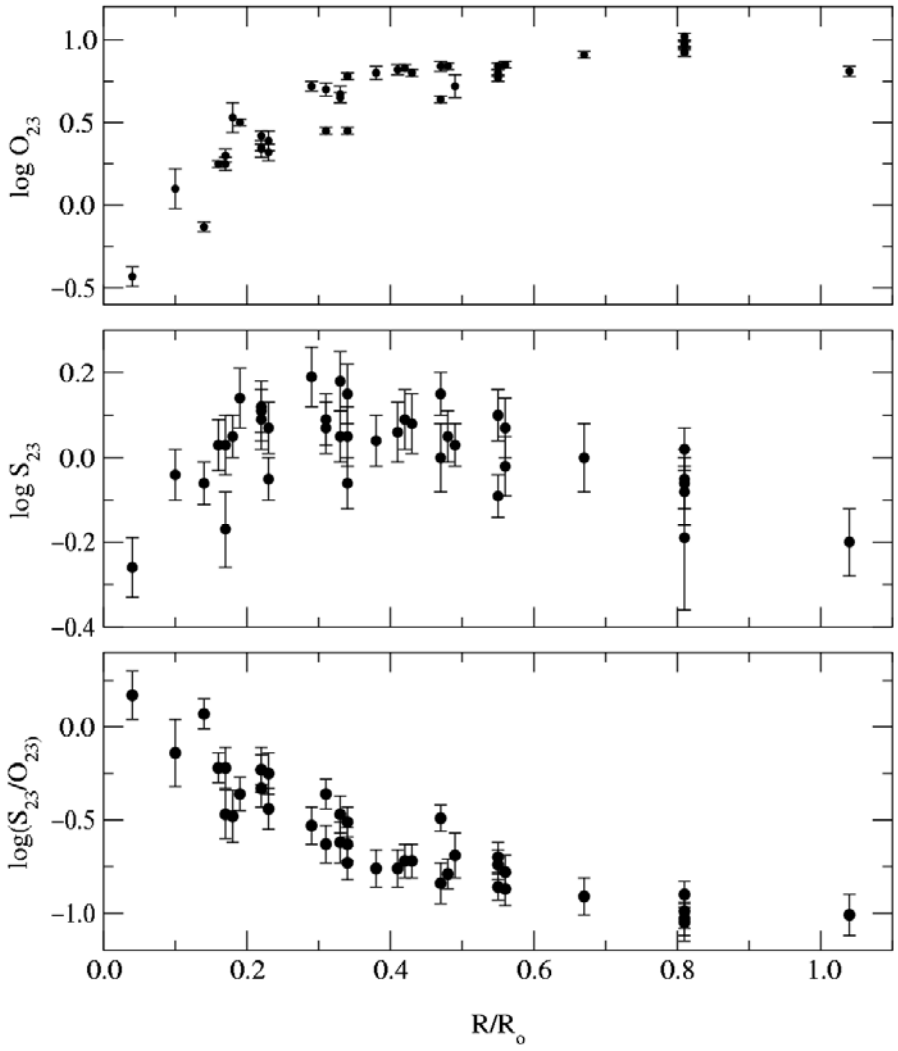

log ([SIII]/[SII])
R/R$_0$
Kennicutt,Bresolin & Garnett 2003
Bresolin 2006

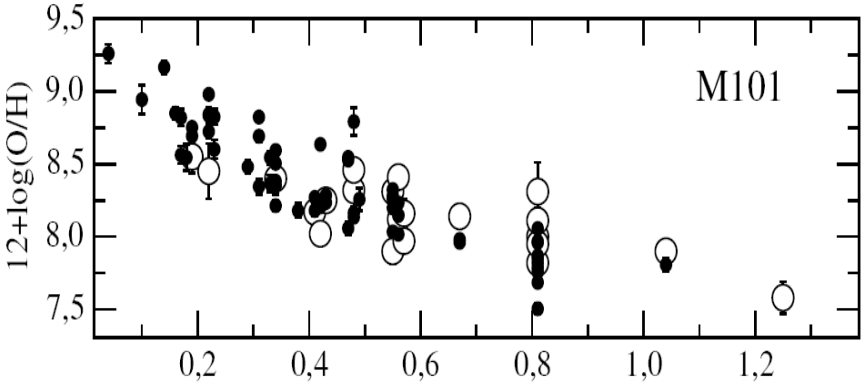

M 101
log(S^{2+}/S^{+})
log([SIII]/[SII])

The S/H abundance gradient in M 101 as derived from direct and empirical methods



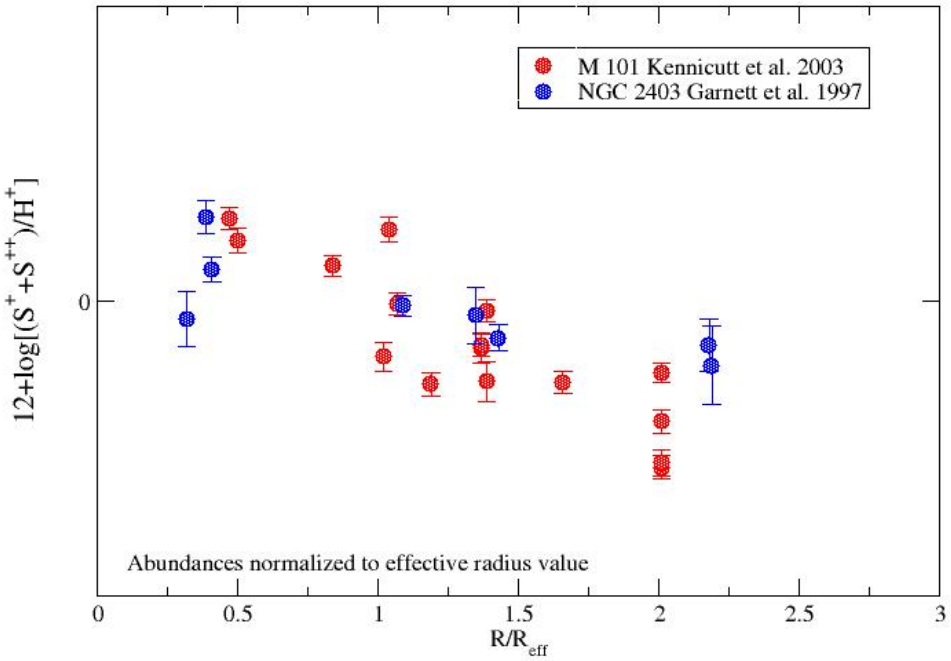
Abundance gradients from empirical indicators





From data of Kennicutt & Garnett (1996) and Kennicutt et al. (2003)

The S gradient for M 101 and NGC 2403



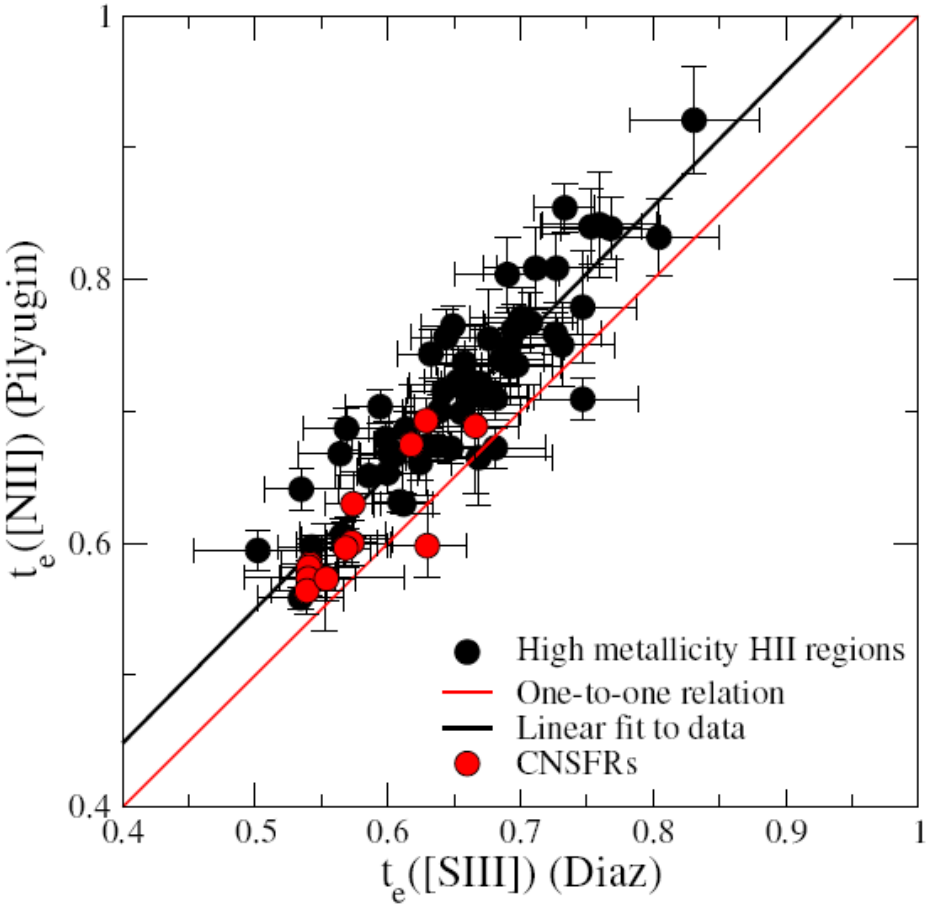
Conclusions

- The use of S as abundance tracer in galaxies presents several important advantages both theoretical and observational.
- In the case of HII galaxies, S abundances can be derived from observations of the 6000 – 10000 Å. It also provides a linear empirical calibration through the S_{23} parameter.
- For the highest excitation regions ICF are required. More work is needed both observational (10.4 μm [SIV]) and theoretical (photo-ionization) models.

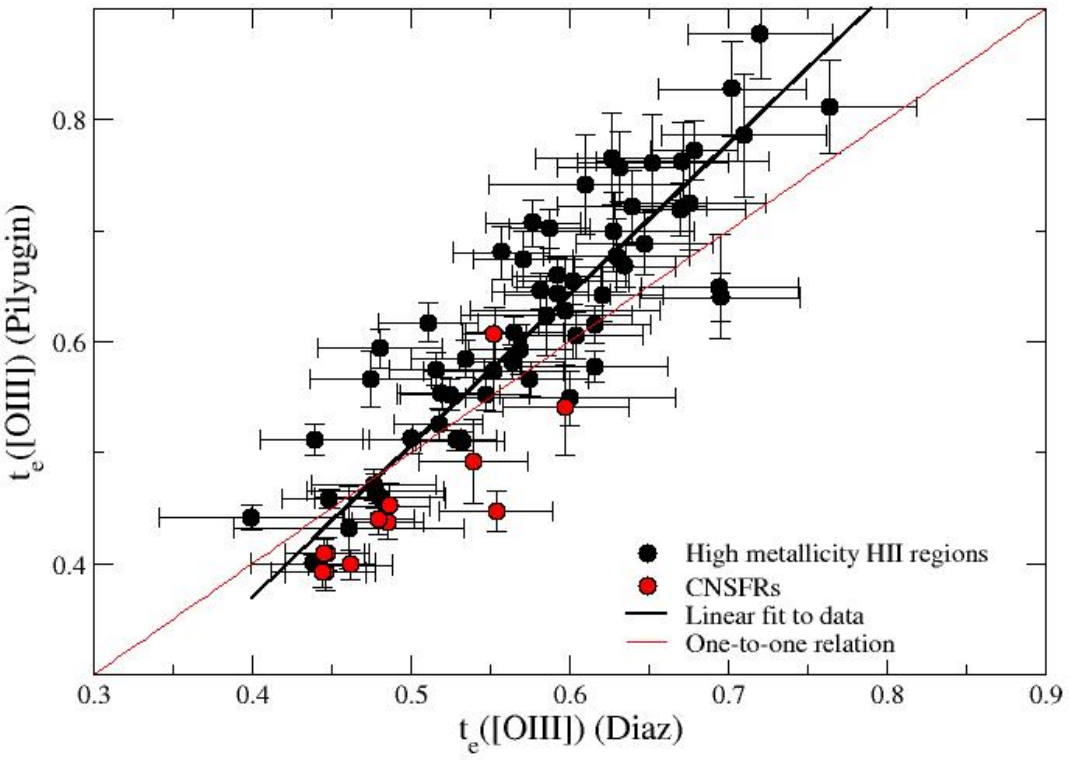
Conclusions

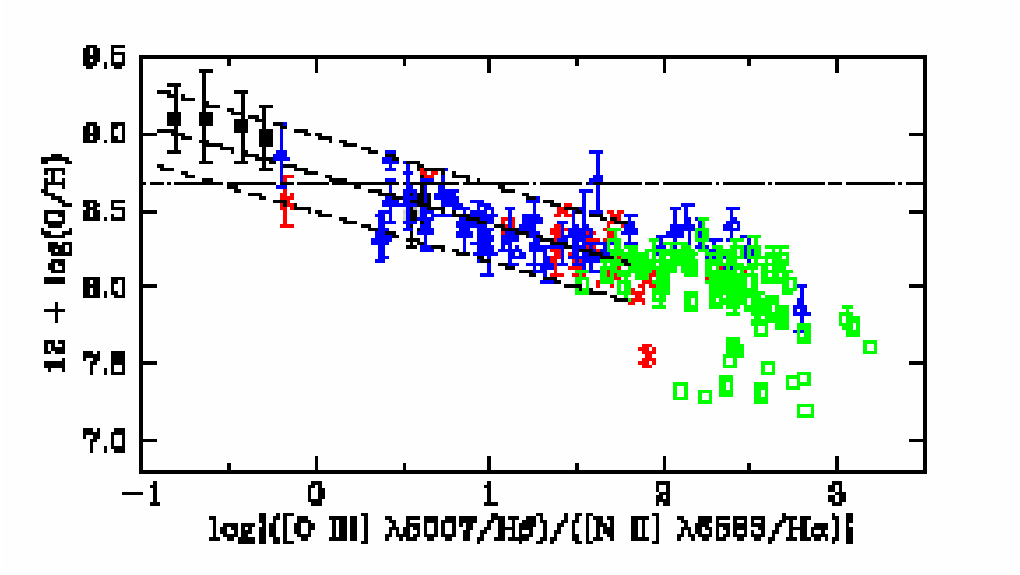
- For high metallicity regions, observations of both O and S lines together, can provide a way to derive abundance values.
- But more work is needed in order to understand the behaviour of S in regions of the highest metallicity.
- In the case of gradients, the run of T_e([SIII]), [SII]/[SIII] (ioniation parameter indicator), and S/H with radius can be found from observations of the 6000 – 10000 Å.
- Empirical indicators provide the same gradient value as derived from direct abundance determinations (but only two galaxies observed!).

Comparison with Pilyugin's method

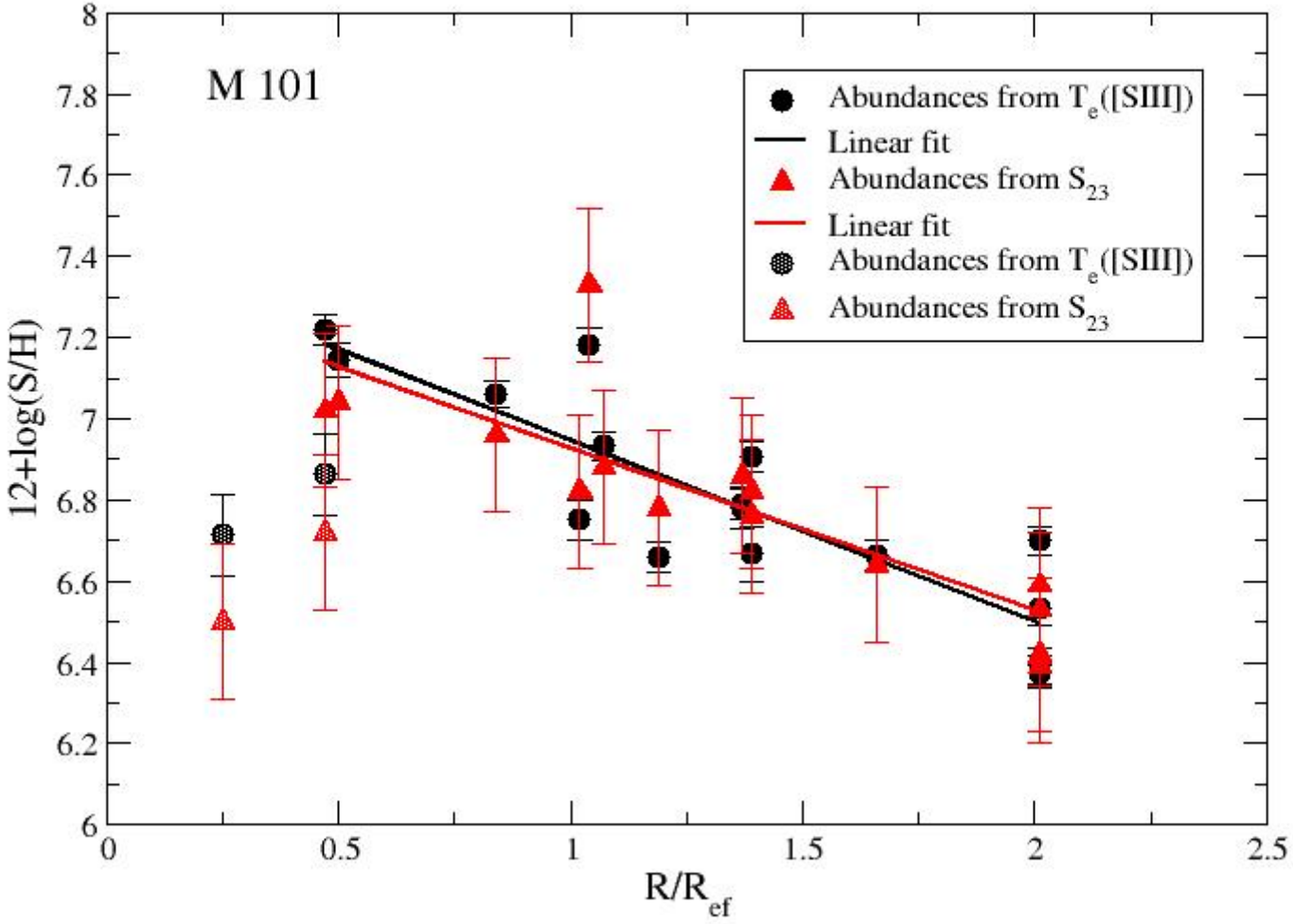


Comparison with Pilyugin's method





Pettini & Pagel (2004)


M 101
Abundances from T_e([SIII])
Linear fit
Abundances from S_{23}
Linear fit
Abundances from T_e([SIII])
Abundances from S_{23}
12+log(S/H)
R/R_{ef}
8
7.8
7.6
7.4
7.2
7
6.8
6.6
6.4
6.2
6
0
0.5
1
1.5
2
2.5